

© 2017 IEEE. Personal use of this material is permitted. Permission from IEEE must be obtained for all other uses, in any current or future media, including reprinting/republishing this material for advertising or promotional purposes, creating new collective works, for resale or redistribution to servers or lists, or reuse of any copyrighted component of this work in other works.

Digital Object Identifier (DOI): 10.1109/APEC.2017.7931181

IEEE Applied Power Electronics Conference and Exposition

A family of series-resonant dc-dc converter with fault-tolerant capability

Levy Ferreira Costa

Giampaolo Buticchi

Marco Liserre

Suggested Citation

L. F. Costa, G. Buticchi and M. Liserre, "A family of series-resonant dc-dc converter with fault-tolerant capability," 2017 IEEE Applied Power Electronics Conference and Exposition (APEC), Tampa, FL, 2017, pp. 3378-3384.

A Family of Series-Resonant DC-DC Converter with Fault-Tolerant Capability

Levy F. Costa, Giampaolo Buticchi and Marco Liserre
Christian-Albrecht-University of Kiel (Uni-Kiel) / Power Electronics Chair (PE)
Kaiserstr. 2, 24143, Kiel, SH, Germany
Email: {lfc,gibu, ml}@tf.uni-kiel.de

Abstract—The Series-Resonant dc-dc converter (SRC) is widely applied in a large range of voltage and power. In most applications, fault tolerance is a highly desired feature and it is obtained through redundancy. This paper proposes a fault tolerance solution for the SRC, which could drastically reduce the need of redundancy. Using the proposed scheme, the full-bridge based SRC or multilevel based SRC can be reconfigured in a half-bridge topology, in order to keep the converter operational even with the failure (open circuit or short circuit) of one switch. Since the proposed scheme can be applied to the FB-SRC and multilevel SRC, a family of fault-tolerant converters is proposed in this work. The advantage of the proposed approach are: minimum additional hardware and no deterioration of the converter efficiency. The proposed fault tolerant solution was experimentally tested in a 10 kW SRC prototype with input/output voltage of 700 V/600 V. A short-circuit fault in a semiconductor is tested and the results confirm the effectiveness of the proposed approach.

Index Terms—Dc-dc converter, fault tolerance, multilevel topologies, reliability.

I. INTRODUCTION

The series-resonant dc-dc converter (SRC) has been used in a wide range of voltage and power applications. In some application, such as Smart Transformer [1], [2], telecommunication or even in renewable energy system, the continuity of operation is of paramount importance. For that reason, a highly reliable system (preferably with redundancies) is required. The fault tolerant feature contributes to increase the availability of the system and several fault tolerance methods have been proposed in literature [3]–[6]. The majority of these methods include a significant amount of extra hardware (such as semiconductors/leg redundancy [3], [5] or series connection of fuses/switches to isolate the fault [3], [4], [6]), increasing the cost and compromising the efficiency of the system. In this context, this paper proposes a fault tolerance solution with minimum additional hardware and no impact on efficiency for the SRC converter, using the inherent fault tolerant capability of this topology. The proposed fault tolerant solution has been briefly introduced in [7] for the unidirectional topology of the full-bridge converter and in this paper it is extended to the SRC based on multilevel topologies.

The generic scheme of the SRC is depicted in Fig. 1 and the primary side bridge can be implemented with a half-bridge, full-bridge or even multilevel topology, as those presented in Fig. 2. The proposed fault tolerant scheme consists in reconfiguring the full-bridge SRC (FB-SRC) or the multilevel

SRC in a half-bridge SRC (HB-SRC) converter. Hence, the proposed approach can be applied to those topologies presented from Fig. 1 (c) to (f). Nevertheless, the output voltage generated by the HB-SRC is half of the output generated by the FB-SRC or the multilevel SRC, considering the same parameters (input voltage, transformer turn ratio, etc). Therefore, a reconfigurable rectifier based on the voltage-doubler topology is used in order to keep the same output voltage. Finally, a family of series-resonant converters based on four different topologies is proposed in this paper. The operation principle of the HB-SRC, FB-SRC and multilevel SRC operating in discontinuous conduction mode (dcm) are presented in Section II. In Section III, the reconfiguration scheme is described in detail for each of the mentioned topologies. The re-configurable rectifier used on the proposed converters is introduced in section IV, and then the proposed fault tolerant converters based on the SRC are presented in this section. Finally, experimental results are provided in Section V, validating the theoretical analysis developed in this paper, and the conclusion is presented in Section VI.

II. SERIES-RESONANT CONVERTER: TOPOLOGIES AND OPERATION PRINCIPLE

Fig. 1 shows the generic scheme of the SRC converter, while Fig. 2 shows possible topologies used to implement the SRC, i.e. half-bridge, full-bridge or even multilevel converter configurations. More specifically, the feasible topologies to be used as an active bridge in the primary side are: half-bridge with dc output (HBdc-SRC, Fig. 2 (a)), classic half-bridge (HB-SRC) with ac output (Fig. 2 (b)), full-bridge (FB-SRC, Fig. 2 (c)), flying-capacitor (FC-SRC, Fig. 2 (d)), 3-level converter (3L-SRC, Fig. 2 (e)) and finally the neural-point-clamped (NPC-SRC, Fig. 2 (f)). Concerning the nomenclature, the topologies based on two switches (Half-Bridges Fig. 2 (a) and (b)) are defined as basic topologies, while the topologies based on four switches (FB Fig. 2 (a) and multilevel Fig. 2 (d) to (e)) are defined as reconfigurable topologies.

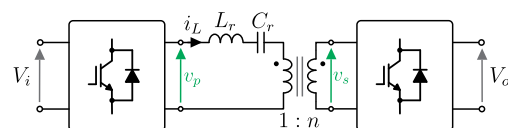


Figure 1. Topology of the series resonant dc-dc converter.

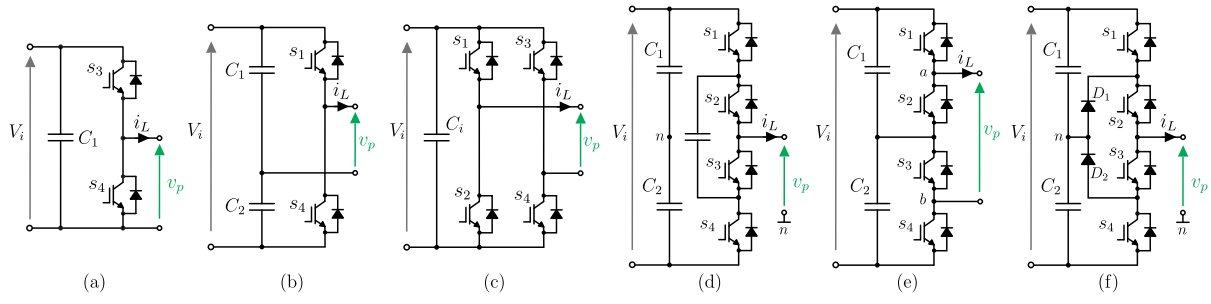


Figure 2. Possible topologies used to implement the active bridges of the series-resonant converter: (a) half-bridge with dc with dc output (HBdc-SRC), (b) classic half-bridge (HB-SRC) with ac output, (c) full-bridge (FB-SRC), (d) flying-capacitor (FC-SRC), (e) 3-level topology (3L-SRC) and (f) neutral-point-clamped (NPC-SRC)

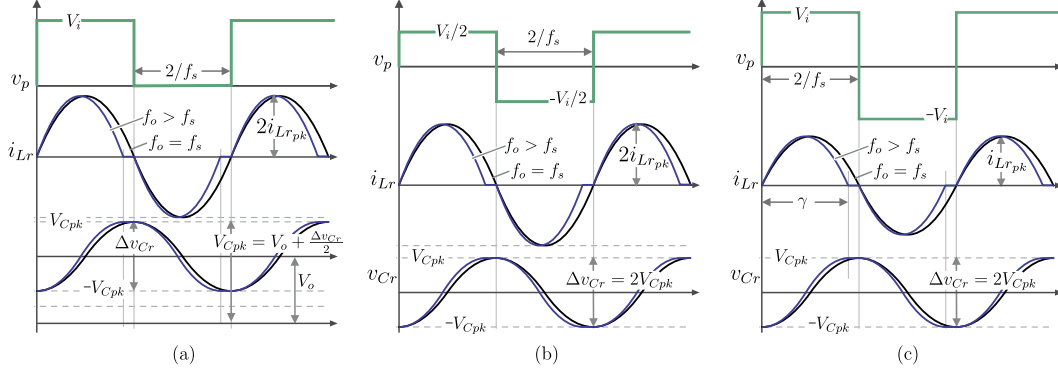


Figure 3. Main waveforms of the SRC for the different topologies implementation: (a) HBdc-SRC, (b) HB-SRC, (c) FV-SRC and multilevel topologies (FC-SRC, 3L-SRC, NPC-SRC).

Although the multilevel converters or even the FB-SRC can work with 3 level modulation (creating a v_p voltage with 3 levels), the 2 level modulation is very beneficial, because it combines the advantages of the SRC converter, that are: high efficiency, well regulated output voltage, low EMI emission (reduced di/dt), with the advantage of the multilevel structure of reducing the voltage effort across the semiconductors. Therefore, the 2 level modulation is used in this work for the FB-SRC and multilevel SRC and the main waveforms for these converters are depicted in Fig. 3 (c).

A. FB-SRC and Multilevel SRC

The FB-SRC and Multilevel SRC operates with 2 level modulation, generating then a 2 level square waveforms v_p on the resonant tank circuit with magnitude varying from V_i to $-V_i$, as depicted in Fig. 3 (c), where V_i is the dc value of the input source. It is desired that the converter operates with switching frequency equal to the resonant frequency, given by (1), ($f_s = f_o$), or slightly above ($f_s > f_o$) [8], [9]. In that condition, the converter will operate with zero-voltage-switching (ZVS) on the primary side and zero-current-switching (ZCS) on the secondary side. For $f_s = f_o$, the resonant inductor current i_{Lr} and resonant capacitor voltage v_{Cr} fully resonate, resulting in pure sinusoidal waveforms. In case of $f_s > f_o$, the inductor current reaches zero before half of the switching period, and it remains zero until the primary bridge applies

negative output voltage $v_p = -V_i$. Since the commutations take place when $i_{Lr} = 0$, all semiconductors switch at ZCS. The main waveforms for both operation point are shown in Fig. 3 (c). In these operation modes, the converter works with unity gain and, then the output voltage is given by (2).

$$f_s = f_o = \frac{1}{2\pi\sqrt{L_r C_r}} \quad (1)$$

$$V_o = n \cdot V_i \quad (2)$$

B. HB-SRC and HBdc-SRC

Similarly to FB-SRC, the HB-SRC (Fig. 2 (b)) generates an ac square waveforms v_p on the resonant tank circuit, but in this case the magnitude varies from $V_i/2$ to $-V_i/2$, because of the half-bridge configuration. Consequently, the inductor current will be two times the one of the FB configuration with the same output power. The main waveforms for this converter are shown in Fig. 3 (b), in which a similar operation to the FB-SRC is observed. The output voltage of the HB-SRC is given by (3). As it can be seen, the output voltage of the HB-SRC is half of the value, when compared to the FB-SRC output voltage (see (2)) for the same parameters (V_i and n).

$$V_o = n \cdot \frac{V_i}{2} \quad (3)$$

Differently from the FB-SRC and HB-SRC, the HBdc-SRC (Fig. 2 (b)) generates a dc value in the voltage v_p on the

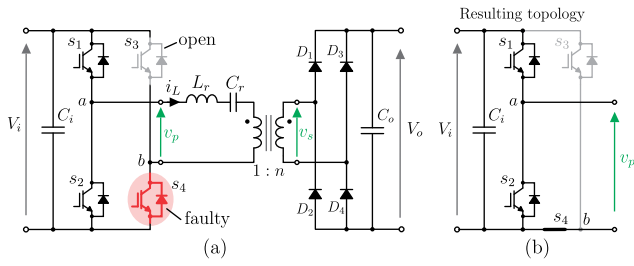


Figure 4. (a) FB-SRC under faulty condition: SC failure on the semiconductor s_4 , (b) resulting topology after the reconfiguration of the FB-SRC.

tank circuit input, with zero and positive values ($0, V_i$). As a consequence of this dc voltage, the resonant tank voltage will have a dc value given by V_o . Similarly to the HB-SRC, the output voltage of the HBdc-SRC is defined by (3) and its inductor current is twice the one of the FB configuration for the case of same output power.

III. PROPOSED FAULT TOLERANCE APPROACH

Depending on the semiconductors failure mechanisms, the device will assume two possible states: open-circuit (OC) or short-circuit (SC) [10]. For a voltage source converter, which is the case of the SRC, the OC fault is not catastrophic, since the power transfer will be naturally interrupted. Instead, the SC fault is the main issue, because it can cause destructive damage to the power converter. In addition, the SC failure type is more likely to happen in the real application than the OC failure. The proposed approach can be applied for both cases, but this work is focused on the SC fault, in which the theoretical analysis will be carried out.

A. Reconfiguration Scheme: Full-Bridge SRC

The proposed reconfiguration scheme for the SRC consists in configuring the FB-SRC in a HB-SRC after the fault, i.e. SC of a semiconductor. The detailed analysis is carried out in this section for the FB-SRC shown in Fig. 2 (c).

As an example, it is assumed that the switch s_4 is damaged in SC, as depicted in Fig. 4 (a), and the switch s_3 must remain open, avoiding short-circuit of the input voltage source. Since the switch s_4 is short-circuited, the point b highlighted in Fig. 4 (a) is directly connected to the primary side ground and the damaged device is used as a circuit path, resulting in the circuit shown in Fig. 4 (b). Meanwhile, the healthy leg (composed of s_1 and s_2) operates normally. As can be noticed, the resulting circuit after the fault (see Fig. 4 (b)) is the same HBdc shown in Fig. 2 (a). Hence, the FB-SRC operates as a HBdc-SRC after the semiconductor fault. Fig. 5 shows the operation states of the SRC after the fault, i.e. after the reconfiguration, where it can be seen that the damaged switch s_4 being used as a circuit path.

B. 3-Level SRC

As mentioned before, the proposed fault tolerant scheme can also be applied to those multilevel topologies depicted in

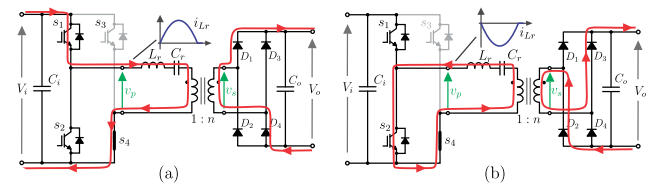


Figure 5. Operation of the FB-SRC as a HBdc-SRC after the reconfiguration. States operation of the SRC after the fault: (a) positive i_L current (first state), (b) negative i_L current (second state).

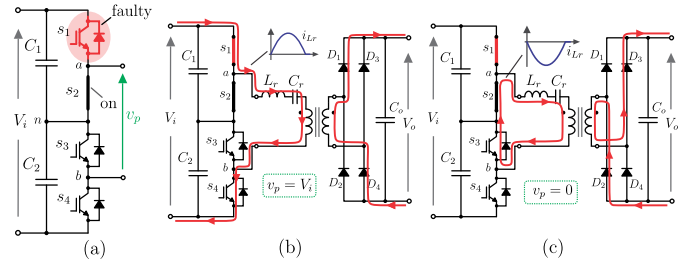


Figure 6. (a) 3L-SRC under faulty condition: SC failure on the semiconductor s_1 . Operation of the 3L-SRC as a HB-SRC after the reconfiguration and the operation states: (b) positive i_L current (first state), (c) negative i_L current (second state).

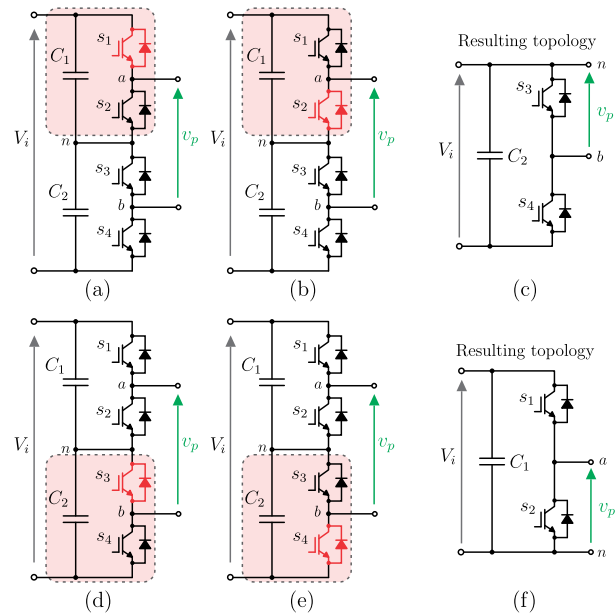


Figure 7. Proposed reconfiguration scheme for the 3L-SRC for a faulty case in every device and the resulting circuit after the reconfiguration: (a) fault in s_1 , (b) fault in s_2 , (c) resulting circuit (HBdc-SRC) after the reconfiguration in case of fault in s_1 or s_2 , (d) fault in s_3 , (e) fault in s_4 , (f) resulting circuit (HBdc-SRC) after the reconfiguration in case of fault s_3 or s_4 .

Table I
SWITCHING STATES FOR THE RECONFIGURATION SCHEME FOR THE 3-LEVEL SRC

Faulty Device	s_1	s_2	s_3	s_4
s_1	SC	ON	switching	switching
s_2	ON	SC	switching	switching
s_3	switching	switching	SC	ON
s_4	switching	switching	ON	SC

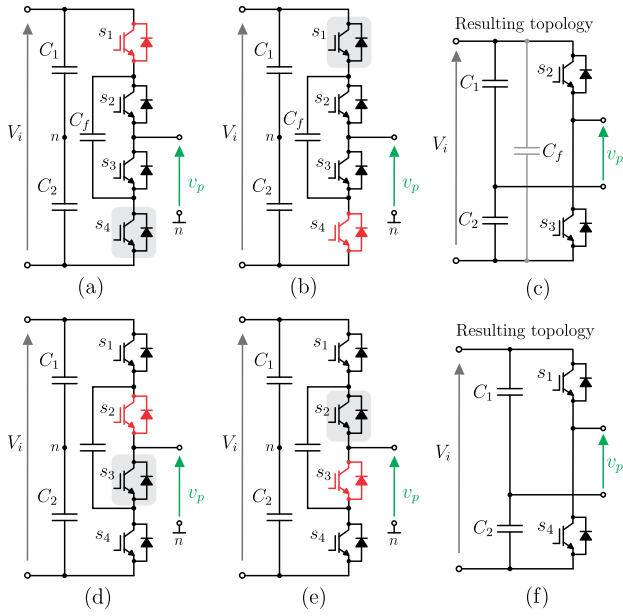


Figure 8. Proposed reconfiguration scheme for the FC-SRC for a faulty case in every device and the resulting circuit after the reconfiguration: (a) fault in s_1 , (b) fault in s_2 , (c) resulting circuit (HB-SRC) after the reconfiguration in case of fault in s_1 or s_2 , (d) fault in s_3 , (e) fault in s_4 , (f) resulting circuit (HB-SRC) after the reconfiguration in case of fault s_3 or s_4 .

Table II
SWITCHING STATES FOR THE RECONFIGURATION SCHEME FOR THE FC-SRC

Faulty Device	s_1	s_2	s_3	s_4
s_1	SC	switching	switching	ON
s_2	switching	SC	ON	switching
s_3	switching	ON	SC	switching
s_4	ON	switching	switching	SC

Fig. 2 (d) to (f) and this section the proposed approach is described for the 3-Level topology (Fig. 2 (e)).

As an example, considering a failure on the switch s_1 , the switch s_2 should be permanently on, as shown in Fig. 6 (a), discharging completely the capacitor C_1 . Then, the part of the circuit composed by C_1 , s_1 and s_2 and highlighted in Fig. 7 (a) is completely by-passed, resulting in the circuit in Fig. 7 (c). The healthy leg composed of s_3 and s_4 operates normally. As observed, the resulting circuit after the fault (see Fig. 7 (c)) is the same HBdc topology shown in Fig. 2 (a), but with the transformer connected to the positive terminal of the input source V_i , instead of the ground. Nevertheless, the modified connection has no influence on the converter operation. Fig. 5 (b) and (c) shows the operation states of the 3L-SRC after the reconfiguration.

The reconfiguration procedure for a failure on the other switches of the 3-Level topology is also presented in Fig. 7, while Table I describes the final state for every remaining healthy switch after the failure on each device.

C. Flying-Capacitor SRC

Similarly to the 3-Level converter, the Flying-Capacitor topology can also take advantage of the proposed fault tolerant

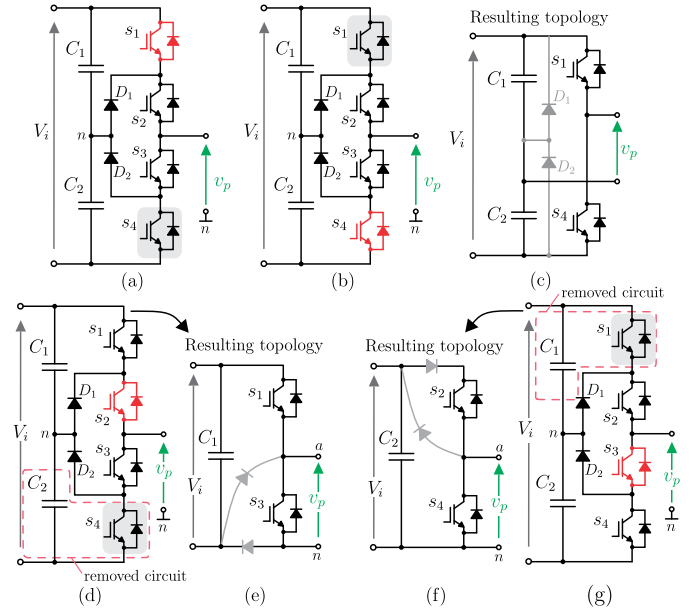


Figure 9. Proposed reconfiguration scheme for the NPC-SRC for a faulty case in every device and the resulting circuit after the reconfiguration: (a) fault in s_1 , (b) fault in s_2 , (c) resulting circuit (HB-SRC) after the reconfiguration in case of fault in s_1 or s_2 , (d) fault in s_3 , (e) fault in s_4 , (f) resulting circuit (HB-SRC) after the reconfiguration in case of fault s_3 or s_4 .

Table III
SWITCHING STATES FOR THE RECONFIGURATION SCHEME FOR THE NPC SRC

Faulty Device	s_1	s_2	s_3	s_4
s_1	SC	switching	switching	OFF
s_2	switching	SC	switching	OFF
s_3	OFF	switching	SC	switching
s_4	OFF	switching	switching	SC

method and the reconfiguration procedure is presented in Fig. 8, as well as the resulting circuit after the reconfiguration, for the faulty case in each switch. Considering a fault on the switch s_1 as an example, the switch s_4 should remain permanently on for the reconfiguration process. Then, the capacitor C_f will be charged with the full dc-link voltage V_i (operating in parallel with the array composed by C_1 and C_2). The switches s_2 and s_3 operate normally and the resulting circuit is shown in Fig. 8 (c). Differently from the FB-SRC and 3L-SRC, the resulting circuit after the reconfiguration of the FC-SRC is the HB-SRC with ac input, shown in Fig. 2 (b). It is important to note that the reconfigurable circuit for the 3L-SRC has better performance compared to the FB-SRC or 3L-SRC, since the resonant capacitor will not operate with a dc voltage after the fault (see Fig. 3 (a) and (b)). Therefore, for the FC-SRC, the reconfiguration has no impact on the resonant capacitor. Table II describes the final state for every remaining healthy switch after the failure on each device.

D. Neutral Point Clamped SRC

Finally, the reconfiguration scheme for the NPC-SRC is described. For this converter, there are two fault possibilities that

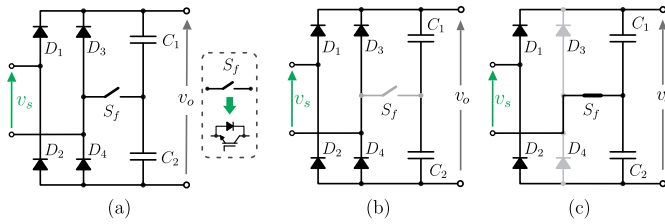


Figure 10. Topology of the re-configurable rectifier (a) and its operation possibilities: (b) operation as a FBR, (c) operation as a VDR.

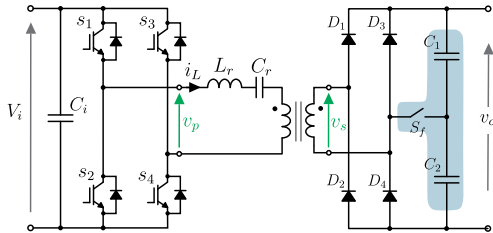


Figure 11. Topology of the proposed fault-tolerant FB-SRC.

will result in two different topologies after the reconfiguration: the first case is for a fault in the outer semiconductors, i.e. s_1 and s_4 , whereas the second case is for inner semiconductors s_2 and s_3 . The reconfiguration procedure of the NPC-SRC for both cases are presented in Fig. 9, as well as the resulting circuit after the reconfiguration, for the faulty case in each switch.

Analyzing the first case, a SC fault on the switch s_1 is assumed as an example, hence the switch s_4 must remain permanently on for the reconfiguration. Consequently, the point a , highlighted in Fig. 9 (a), is connected to the positive terminal of the input dc-link V_i , whereas the point b (see Fig. 9) is connected to the ground, bypassing the clamp diodes D_1 and D_2 and resulting in the circuit shown in Fig. 9 (c). Meanwhile, the healthy switches s_2 and s_3 operate normally. Similarly to the FC-SRC, the resulting circuit for the first fault case of the NPC-SRC is a HB-SRC.

Evaluating the second case, a fault on the switch s_2 is assumed and, as part of the reconfiguration process, the switch s_4 must remain open. Furthermore, the part of the circuit composed by the capacitor C_2 and s_4 is removed from the topology, resulting in the circuit shown in Fig. 9 (e). Thus, differently from the previous case, the resulting circuit after the reconfiguration is a HBdc-SRC. Table III describes the final state for every remaining healthy switch after the failure on each device.

IV. PROPOSED FAMILY OF FAULT-TOLERANT SERIES-RESONANT CONVERTER

As described in previous sections, using the proposed fault tolerance approach, the FB-SRC and multilevel SRC are reconfigured in the basic HB-SRC and HBdc-SRC topologies. On the other hand, it is important to note that the HB-SRC and the HBdc-SRC provide only half of the output voltage

compared to the FB-SRC and multilevel SRC topologies. Consequently, the output voltage of the re-configurable converters after the fault will be half of its original value, which is not desired. To overcome this problem and keep the output voltage constant after the failure, a re-configurable rectifier introduced in [7] is used.

The full-bridge rectifier (FBR) topology is the most used in the secondary side of the SRC [11], [12]- [13], as depicted in Fig. 4 and Fig. 6. The voltage-doubler rectifier (VDR), which is also popular in the literature, can also be used in the SRC. While the FBR provides an output dc voltage of $v_o = v_{s_{pk}}$, where $v_{s_{pk}}$ is the effective voltage generated on the secondary side of the transformer, the VDR provides an output dc voltage of $v_o = 2 \cdot v_{s_{pk}}$.

In this context, the voltage doubler characteristic of the VDR can be used to keep the output voltage of the reconfigurable converters constant in case of fault. Thus, a re-configurable rectifier able to operate as a FBR or a VDR, previously introduced in [7], is employed to overcome the drawback of the proposed approach. The re-configurable rectifier circuit is presented in Fig. 10 (a). As can be seen in this figure, the re-configurable rectifier has two split capacitors and an additional switch (S_f) that allows to connect one side of the high frequency transformer secondary winding directly to the middle point of the capacitors, becoming a VDR.

The operation in normal and faulty conditions is depicted in Fig. 10 (b) and Fig. 10 (c), respectively. In normal operation, the switch S_f is open, and the rectifier operates as a standard FBR. In fault case, the switch S_f is activated, and then the leg composed of the diodes D_3 and D_4 is bypassed. The bottom side of the secondary winding is connected to the middle point of the capacitors C_1 and C_2 , becoming an VDR. Therefore, the circuit operates as a VDR, and the output voltage value is twice the output voltage value in normal operation.

Finally, a family of fault tolerant series resonant converter based on the FB and multilevel topologies (previously depicted in Fig. 2 (c) to (f)) is generated, as shown in Fig. 11 and in Fig. 12. Fig. 11 shows the complete topology of proposed fault tolerant FB-SRC, while the Fig. 11 shows the topologies of the proposed fault tolerant multilevel SRC.

V. EXPERIMENTAL VALIDATION OF THE PROPOSED APPROACH

In order to verify the performance of the proposed fault tolerance approach, a prototype of 10 kW was built and experimental results were obtained. As a matter of simplicity, the FB-SRC presented in Fig. 11 was chosen to be implemented and evaluated experimentally. The specifications of the implemented power converter prototype, as well as the resonant tank circuit parameters are presented in Table IV. The IGBT IHW40N120 (1200V/40A, from *Infineon Technologies AG*) was selected as the main switch and it was used on the primary side and secondary sides. For the secondary side, the intrinsic diodes of the IGBT were used to rectifier. The converter operates in open loop and the gating signals are generated by the DSP. To evaluate dynamically the performance of the

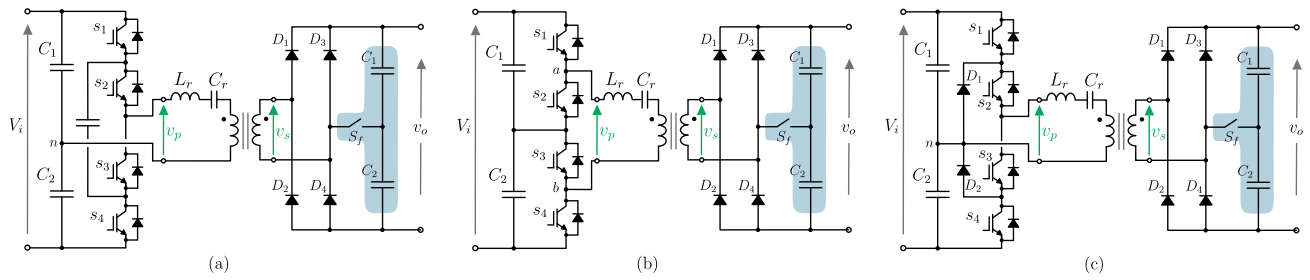


Figure 12. Proposed fault-tolerant series resonant dc-dc converter based on the multilevel topologies: (a) fault-tolerant FC-SRC (FT-FC-SRC), (b) fault-tolerant 3L-SRC (FT-3L-SRC), (c) fault-tolerant NPC-SRC (FT-NPC-SRC).

converter under fault case, a short-circuit on the switch s_2 was emulated by software in the DSP.

Fig. 13 shows the photo of the prototype and the main waveforms for the converter operating in steady-state at nominal condition. The results were obtained for the converter operating in steady-state (before and after the fault) and also dynamically during the fault and they are discussed herein. For safety reasons, the dynamic results were obtained for reduced input and output voltages.

Initially, the converter was tested considering only the reconfiguration scheme in the primary bridge, without the reconfigurable rectifier, with the aim of validating the fault tolerant approach and the reconfiguration methodology described in Section III. The test was performed with input and output voltage of 200 V and 300 V, respectively, and the result for this condition is presented in Fig. 14 (a). In this figure, it is observed the dynamic response of the FB-SRC during the fault of the switch s_2 , in which the converter remains operational after the fault, proving its inherent ability to handle the fault. As expected, the output voltage drops to half of its value (from 300 V to 150 V) after the fault and the capacitor voltage has an offset of V_o . The inductor current is also reduced, because the test was performed with constant resistance as load and therefore reduction on the output voltage implies in reduction on power.

Subsequently, the prototype was tested including the reconfigurable rectifier, in order to validate the operation of the proposed fault-tolerant FB-SRC topology. For this test, it was considered an input voltage of 350 V and output voltage of 500 V, and the main results are presented from Fig. 14 (b) to (d). The dynamic behavior during the fault on switch s_2 is depicted in Fig. 14 (c), showing that the converter remains operational after the failure. Additionally, the converter provides a constant output voltage (500 V) even after the fault, attesting the effectiveness of the proposed rectifier and the converter. As the output voltage remains constant, the amount of processed power is the same before and after the fault and therefore the amount of current on the resonant tank is twice after the fault, as previously described. The detailed waveforms before and after the fault can be observed in the Figs. 14 (c) and (d), respectively. As can be observed in these figures, the converter behaves as a FB-SRC before the fault and as a HBdc-SRC after the fault, and the experimental waveforms (Figs. 14 (c) and

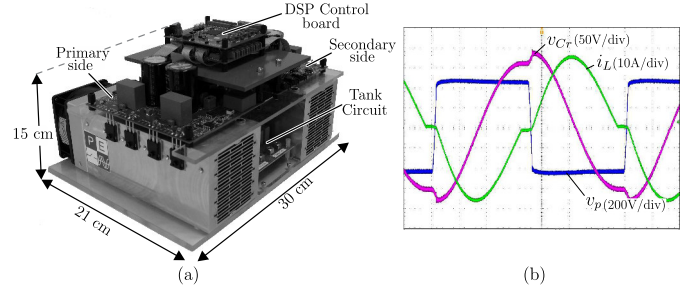


Figure 13. Implemented 10 kW fault tolerant SRC converter hardware prototype: (a) photo of the prototype (mechanical dimensions: 300 mm x 210 mm x 150 mm: power density: 1 kW/dm³), (b) experimental result at nominal load ($V_i = 700$ V, $V_o = 600$ V, $P_o = 10$ kW), showing the operation of the prototype.

Table IV
SPECIFICATION OF THE SRC PROTOTYPE AND THE RESONANT CIRCUIT PARAMETERS

Power converter specification	
Input voltage	$V_i = 700$ V
Output voltage	$V_o = 600$ V
Nominal output power	$P_o = 10$ kW
Switching frequency	$f_s = 20$ kHz
Transformer turn ratio	$n = 1.45$
Resonant circuit parameter	
Resonant capacitance	$C_r = 0.68\mu\text{F}$
Resonant Inductor	$L_r = 79\mu\text{H}$
Tank resonant angular frequency	$\omega_0 = 1.364 \cdot 10^5$ rad/s
Resonant frequency	$f_o = 21.7$ kHz

(d)) are in accordance with the theoretical one shown in Fig. 3 (c) and (a).

To summarize, the results have shown that the proposed converter can handle a short-circuit fault in one device and still provide the required output voltage and power, keeping the continuity of operation.

VI. CONCLUSION

This paper proposed a family of series-resonant dc-dc converter with fault tolerance capability. The proposed fault tolerance method consists in re-configuring the FB-SRC or multilevel SRC in a half-bridge SRC (HB-SRC or HBdc-SRC), in case of a semiconductor failure, keeping the converter operational. The proposed approach can be applied to the

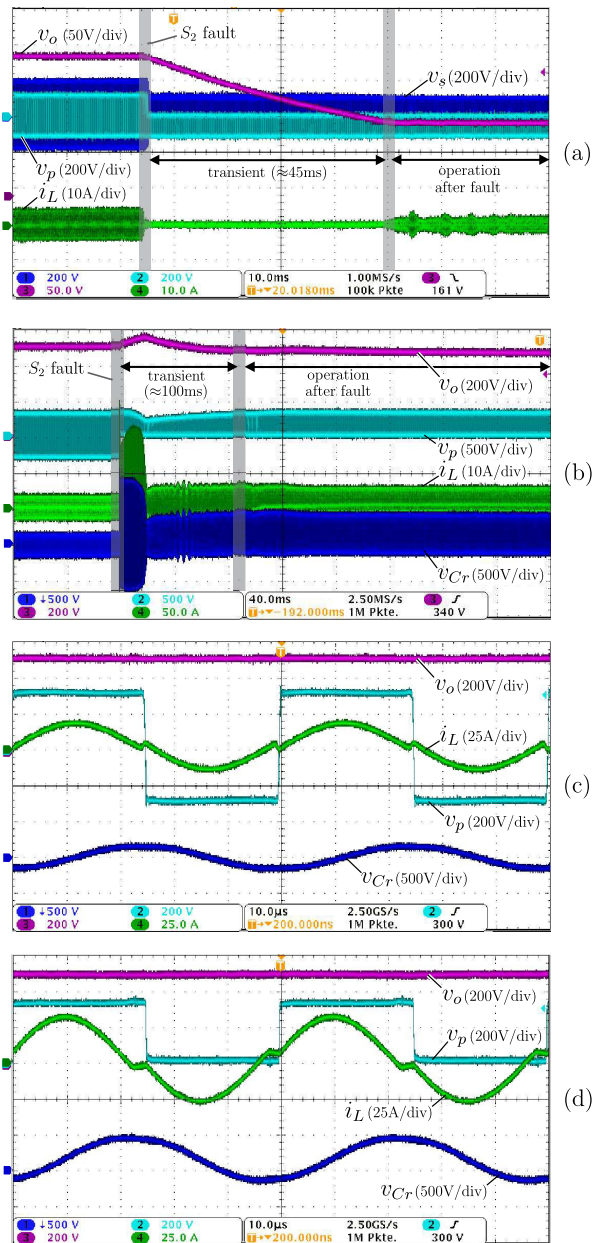


Figure 14. Experimental results of the FB-SRC under a fault on the switch s_2 : (a) dynamic behavior of the converter during the fault, without the reconfigurable rectifier on the secondary side, (b) dynamic behavior of the converter during the fault, including the reconfigurable rectifier, (c) steady-state operation before and (c) after the fault, considering the re-configurable rectifier on the secondary side.

series resonant converter based on full-bridge, three-level, flying capacitor and neutral point clamped topologies, and the reconfiguration methodology for each of them was described. As a result of the reconfiguration, the output voltage is reduced. To overcome this problem a modified rectifier that

can be reconfigured in a voltage doubler rectifier, keeping the output voltage constant, is used. Then, a family of SRC with fault capability is generated and presented.

The main advantages of the proposed converter are: post-fault operation, simple implementation, reduced number of additional component and no efficiency deterioration. As a drawback, the resonant capacitor must be designed for higher voltage and the current effort on the healthy devices in failure mode operation is twice the than in normal mode operation.

Experimental results for a 10 kW prototype were obtained and the effectiveness and advantages of the proposed fault tolerant series resonant dc-dc converter has been demonstrated.

REFERENCES

- [1] M. Liserre, G. Buticchi, M. Andresen, G. D. Carne, L. F. Costa, and Z. X. Zou, "The smart transformer: Impact on the electric grid and technology challenges," *IEEE Industrial Electronics Magazine*, vol. 10, no. 2, pp. 46–58, Summer 2016.
- [2] M. Liserre, M. Andresen, L. F. Costa, and G. Buticchi, "Power routing in modular smart transformers," *IEEE Industrial Electronics Magazine*, 2016 (in press).
- [3] W. Zhang, D. Xu, P. N. Enjeti, H. Li, J. T. Hawke, and H. S. Krishnamoorthy, "Survey on fault-tolerant techniques for power electronic converters," *IEEE Transactions on Power Electronics*, vol. 29, no. 12, pp. 6319–6331, Dec 2014.
- [4] Y. Song and B. Wang, "Survey on reliability of power electronic systems," *IEEE Transactions on Power Electronics*, vol. 28, no. 1, pp. 591–604, Jan 2013.
- [5] E. Ribeiro, A. Cardoso, and C. Boccaletti, "Fault-tolerant strategy for a photovoltaic dc-dc converter," *IEEE Transactions on Power Electronics*, vol. 28, no. 6, pp. 3008–3018, June 2013.
- [6] X. Pei, S. Nie, Y. Chen, and Y. Kang, "Open-circuit fault diagnosis and fault-tolerant strategies for full-bridge dc-dc converters," *IEEE Transactions on Power Electronics*, vol. 27, no. 5, pp. 2550–2565, May 2012.
- [7] L. F. Costa, G. Buticchi, and M. Liserre, "Fault-tolerant series-resonant dc-dc converter," *IEEE Transactions on Power Electronics*, 2016 (in press).
- [8] T. LaBella, W. Yu, J. S. . Lai, M. Senesky, and D. Anderson, "A bidirectional-switch-based wide-input range high-efficiency isolated resonant converter for photovoltaic applications," *IEEE Transactions on Power Electronics*, vol. 29, no. 7, pp. 3473–3484, July 2014.
- [9] T. LaBella and J. S. Lai, "A hybrid resonant converter utilizing a bidirectional gan ac switch for high-efficiency pv applications," *IEEE Transactions on Industry Applications*, vol. 50, no. 5, pp. 3468–3475, Sept 2014.
- [10] R. Wu, F. Blaabjerg, H. Wang, M. Liserre, and F. Iannuzzo, "Catastrophic failure and fault-tolerant design of igbt power electronic converters - an overview," in *Conference of the IEEE Industrial Electronics Society (IECON)*, Nov 2013, pp. 507–513.
- [11] T. Lazzarin, O. Custodio, C. C. Motta, and I. Barbi, "An isolated dc-dc converter with high-output-voltage for a twta," in *International Telecommunications Energy Conference (INTELEC)*, Sept 2014, pp. 1–7.
- [12] M. Petersen and F. Fuchs, "Load dependent power control in series-series compensated electric vehicle inductive power transfer systems," in *European Conference on Power Electronics and Applications (EPE-ECCE Europe)*, Aug 2014, pp. 1–10.
- [13] C. Meyer and R. De Doncker, "Design of a three-phase series resonant converter for offshore dc grids," in *42nd IAS Annual Meeting. Conference Record of the 2007 IEEE Industry Applications Conference*, Sept 2007, pp. 216–223.